

Detecting forced changes in internal variability using Large Ensembles: On the use of methods based on the “snapshot view”

Tímea Haszpra¹, Dániel Topál^{2,3}, Mátyás Herein¹

¹Eötvös Loránd University, Hungary

²Research Center for Astronomy and Earth Sciences, Hungary

³University of California-Santa Barbara, USA

Anthropogenic activities contribute to the rising level of greenhouse gas concentrations in the atmosphere at a rate of approximately 1% per year providing a time-dependent external radiative forcing on the climate system (Peters et al. 2020). Associated changes in several climate variables (e.g., global mean surface temperature) are thought to have emerged from unforced natural internal processes of the climate system allowed by the characteristics of the dissipative chaotic nature of the climate dynamics, i.e., from internal variability (Hawkins et al. 2020). In addition to tangible consequences of anthropogenic forcing affecting the climate system (e.g., the dramatic Arctic sea ice retreat (Screen and Simmonds 2010)), simultaneous, less apparent changes occurring on low-frequency timescales demand effort to deal with. These include changes in internal variability due to the non-stationary anthropogenic forcing, that represents additional uncertainty affecting future model projections on top of internal variability, scenario and model uncertainty (Hawkins and Sutton 2009; Deser et al. 2012; Wettstein and Deser 2014; Lehner et al. 2020).

Although previous studies using observations and multi-model single-member simulations successfully detected, for example, changes in the jet-stream variability (Barnes and Polvani 2013) or in the variance of Northern Hemisphere (NH) temperature (Screen 2014) due to anthropogenic forcing, traditional methods based on long-term temporal statistics unavoidably make use of discrete time windows subjectively chosen from a continuously time dependent system (i.e., the changing climate). In addition, separating the effects of model structural differences and internal variability in multi-model ensembles is challenging (Merrifield et al. 2019). State-of-the-art Single Model Initial-condition Large Ensemble (SMILE) simulations (Kay et al. 2015; Maher et al. 2019; Deser et al. 2020) – that account for the chaotic behavior of the climate system with perturbed initial condition runs of the same model – offer a way forward for new perspectives on externally-forced changes in internal variability. Here, we outline an approach for analyzing SMILEs called the snapshot view, which offers a mathematically exact and elegant formulation and

the potential to complement previous diagnostics with ensemble-based statistics.

Theoretical background – The snapshot view

The concept of the so-called “snapshot view” was introduced into dynamical system theory to understand how nonautonomous dynamics behave when subjected to general time dependent forcings. Romeiras et al. (1990) drew attention to an interesting feature of dissipative dynamical systems: the fact that a single long “noisy” trajectory traces out a fuzzy shape, while an ensemble of motions starting from many different initial conditions, using the same noise realization along each trajectory, creates a structured fractal pattern at any instant. This ensemble-related pattern, the snapshot chaotic attractor, continuously changes its shape, in contrast to traditional chaotic attractors, which are time-independent (Lorenz 1963; Ott 1993). The concept of snapshot attractors has been used to understand a variety of time-dependent physical phenomena (see e.g., Pikovsky 1984; Yu et al. 1990; Serquina et al. 2008; Ku et al. 2015; Vincze et al. 2017). However, it was not until Ghil et al. (2008) and Checkroun et al. (2011) pointed out its potential importance to the field of climate dynamics that it began to be more widely applied in climate science and that this concept (also called the “pullback attractor”) was relevant for the understanding of anthropogenic climate change.

Deterministic (noise-free) snapshot attractors capture the essence of an unpredictable dynamical system under changing conditions (Bódai and Tél 2012; Pierini 2014; Drótos et al. 2015). The traditional way of obtaining a chaotic attractor by means of a “single trajectory” is not equivalent to the “ensemble” method (ergodicity does not hold in systems subjected to forcings of general time-dependence). One has to choose between the two approaches, and it is the ensemble-based snapshot view that is appropriate for a faithful statistical representation of the possible distribution of a given quantity at any time instant in a changing climate. The reason is that the ensemble also represents a natural probability distribution, supported by the snapshot attractor.

The basic features of the snapshot view valid for any dissipative system subjected to general forcing can be summarized as follows (Drótos et al. 2015):

- Conclusions based on single trajectories may be misleading since such trajectories are unpredictable, thus not representative.
- On the contrary, ensemble properties, including the natural probability distributions (which set in after the initial conditions are “forgotten” in a numerical simulation) are fully predictable in a statistical sense (in harmony with general properties of chaotic systems (Tél and Gruiz 2006)).
- An instantaneous characterization of the system becomes possible (as properly expressed by the adjective “snapshot”), and the use of (occasionally biased) temporal averages can fully be avoided.
- It offers a straightforward way to analyze internal variability in a changing system, e.g., by means of statistical quantifiers of the instantaneous probability distribution.
- Because the instantaneous (snapshot) statistics are available at each time instant, the forced changes in any quantity, such as the internal variability, can be determined by analyzing the time series of snapshot values by means of the traditional tools of time series analysis.

In the particular example of climate change, the snapshot view can equivalently be formulated as the theory of *parallel climate realizations* (Herein et al. 2017; Tél et al. 2019). Qualitatively speaking, one can imagine many copies of the Earth system moving on different dynamical paths, each being subjected to the same physical laws and forcings. As a generalization of Leith’s observation (Leith 1978), parallel climate realizations constitute an ensemble of a large number of members, and the snapshot taken over the ensemble (the snapshot attractor) represents the plethora of permitted climate states at that instant.

Utilizing the snapshot view to detect forced changes in internal variability

In this section we reveal how the *snapshot view* allows for surprisingly simple practices to detect forced changes in internal variability via utilizing SMILE simulations. Here, we focus on modes of large-scale internal atmospheric circulation variability (so-called “teleconnection patterns”), which may change due to anthropogenic forcing. The question arises how to characterize changes in these modes as a result of climate change, since certain characteristics of the linkages between the teleconnection patterns and other climate variables, for example precipitation or air temperature, may also change even within a carefully chosen time window (Drótos et al. 2015; Herein et al. 2016; Herein et al. 2017; Tél et al. 2019). Therefore, we need to reconsider these methodologies when aiming to detect forced changes in internal variability.

Our previous research (Haszpra et al. 2020b) exemplified a novel means of analyzing changes in modes of atmospheric circulation variability when the climate system is subjected to time-dependent external forcing, via introducing the snapshot empirical orthogonal function (SEOF) analysis. Rather than apply empirical orthogonal function (EOF) analysis in the traditional temporal dimension we compute instantaneous EOFs (spatial patterns of variability) and associated principal components (PCs, amplitude and polarity of the patterns) across the ensemble dimension. In doing so, we can monitor the changes in an EOF mode resulting from the time-dependent external forcing and account for the non-stationarity of internal variability. We note that a similar method was also developed in Maher et al. (2018), however, that approach combines the variability of the monthly data with that of the ensemble.

The instantaneous strength of the linkage between a particular SEOF teleconnection pattern and another climate variable (e.g., surface temperature, TS) can be quantified by means of the *snapshot correlation*, i.e., the instantaneous Pearson correlation coefficient computed across the ensemble. In this way, instantaneous

correlation maps are obtained, thereby allowing one to monitor the spatial distribution of the correlation field in tandem with its time evolution. Such an approach has been insightful for documenting changes in the teleconnections of the ENSO (Bódai et al. 2020, Haszpra et al. 2020a) and that of the North Atlantic Oscillation (Herein et al. 2017). Similar to EOF analysis, maximum covariance analysis (MCA, Bretherton et al. 1992) may also analogously be extended to its ensemble-based twin (snapshot MCA, SMCA) to study forced changes in coupled modes of variability (see below).

Results

An illustrative example of SEOF: The Arctic Oscillation

We briefly demonstrate advantages of SEOF analysis in monitoring temporal changes in the Arctic Oscillation (AO) under RCP8.5 forcing in the CESM Large Ensemble (CESM-LE, Kay et al. 2015) for 1950–2099. We define the AO as the leading SEOF mode in the winter (December–January–February, DJF) seasonal mean sea level pressure (SLP) anomalies poleward of 20°N and the corresponding PC series as the instantaneous (DJF) AO indices (AOI). Thus, for each winter season during 1950–2099 we obtain a spatial pattern that characterizes the current set of potential climate states (spanned by the ensemble spread) and explains the largest variability in their SLP fields, in addition to a PC series whose length is the number of ensemble members (for the AO, this PC is termed the AO Index or AOI).

The left panel in Figure 1 illustrates the instantaneous DJF mean SLP anomalies regressed onto the leading SEOF mode in 2025 in the CESM-LE, which closely resembles the observed AO pattern (based on historical reanalysis, not shown but see for example Thompson et al. 2000). Repeating the SEOF analysis for each year between 1950–2099, important characteristics of the model’s AO are revealed, including temporal changes in amplitude at several locations determined from a linear fit to the regression values at each grid box (Figure 1 right). For clarity, in this panel dots represent geographical locations

where the linear trend is found to be significant at the 95% level and crosses indicate where, in addition, the regression coefficients are significant at the 95% level in the temporal mean. For example, the amplitude of the AO in the Pacific center-of-action shows an increase of about 0.02 hPa yr^{-1} , implying 3 hPa over 150 years, i.e., the change is of the same magnitude as the typical amplitude in 2025 (2.5–6.5 hPa). On the contrary, in the northern part of Europe and Asia a slight decrease of the AO amplitude can be observed. Moreover, the choice of the scenario influences the magnitude of the changes (see application to the MPI Grand Ensemble (MPI-GE) with three forcing scenarios in Haszpra et al. 2020b).

The AOIs are constructed for each winter season during 1950–2099 by projecting the instantaneous SLP anomalies of the ensemble members onto the given (instantaneous) loading (SEOF) pattern. A rather straightforward step is to calculate the snapshot correlation coefficient r field between the AOI and the surface air temperature (T_s) across the ensemble. In the left panel of Figure 2, the correlation map is shown for 2025. Similar to the SLP regression map, the correlation map resembles the observed relationship between the AO and T_s (Wallace and Gutzler 1981). Fitting a linear trend at each grid point to the time series of snapshot correlation coefficients, significant changes are evident in the strength of the teleconnections across the NH. Dots and crosses in the right panel of Figure 2 indicate regions where the snapshot correlation coefficients undergo significant changes over time, and may need to be taken

into account in future seasonal prediction. These regions include, e.g., Alaska, the eastern part of the Pacific Ocean and Northern Europe where the negative correlations become more pronounced (the correlation coefficient decreases by 0.1–0.3 over 150 years), and a substantial positive trend can be found in the eastern part of Asia where the correlation coefficient increases from about 0.6 to 0.8 over 150 years.

An illustrative example for SMCA: Atmosphere–sea ice coupling under different forcing scenarios

Next, we consider an example from a different season and study how the coupling between the summertime (June–July–August, JJA) Arctic atmospheric circulation and September sea ice variability might depend on future anthropogenic forcing (Ding et al. 2019). Concomitant patterns of high-pressure anomalies in the Arctic and enhanced sea ice melt has been previously shown in SMILEs (Topál et al. 2020), but there has been little focus on possible nonlinearities in the nature or strength of the coupling.

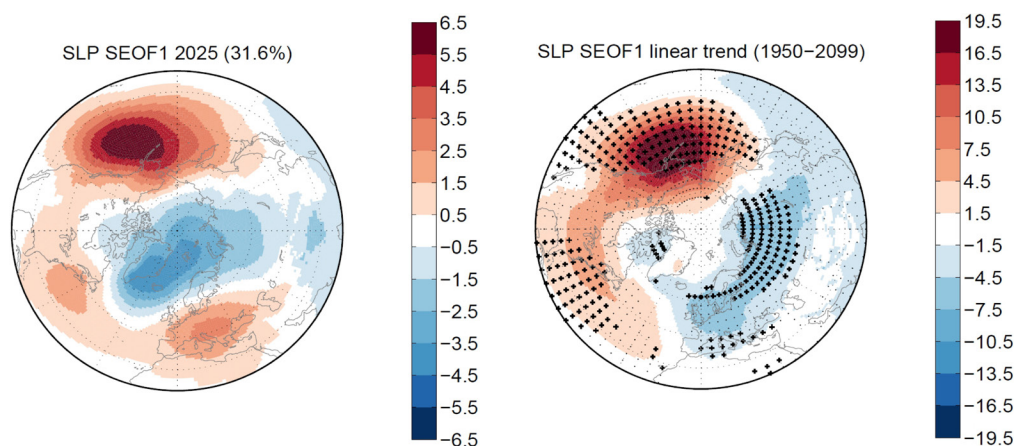


Figure 1. (left) December-January-February (DJF) mean sea level pressure (SLP) anomalies (hPa) regressed onto the first SEOF mode (explained variance is indicated in parenthesis) in 2025 based on the CESM-LE (RCP8.5 scenario). (right) Linear trend ($10^{-3} \text{ hPa yr}^{-1}$) in the SEOF SLP regression coefficients during 1950–2099 based on the CESM-LE under historical and RCP8.5 forcing. Dots represent geographical locations where the trend is significant at the 95% level. Crosses indicate where, in addition, the regression coefficients are significant at the 95% level in the temporal mean.

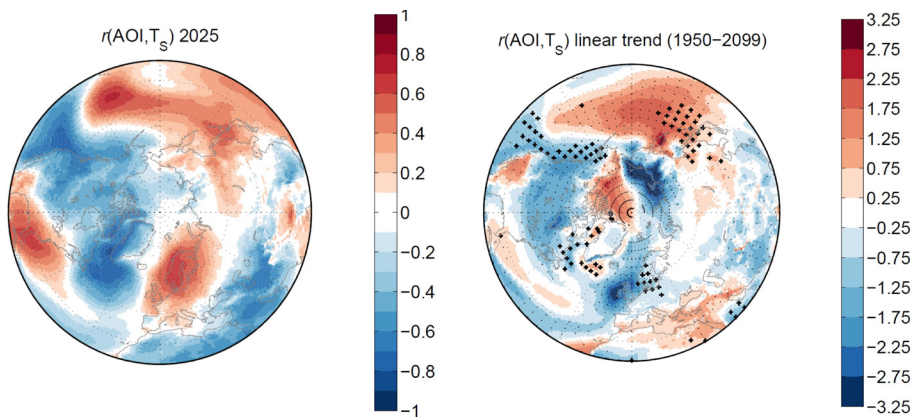


Figure 2. (left) Ensemble-based snapshot correlation coefficient field between the Arctic Oscillation Index and surface air temperature in 2025 based on the CESM-LE (RCP8.5 scenario). (right) Linear trend (10^{-3} yr^{-1}) in the snapshot correlation coefficient during 1950–2099 based on the CESM-LE under historical an RCP8.5 forcing. Dots represent geographical locations where the trend is significant at the 95% level. Crosses indicate where, in addition, the correlation coefficients are significant at the 95% level in the temporal mean.

To study the influence of external forcing on the coupling between the atmospheric circulation and sea ice, we calculate linear trends in all members of each of the three RCP scenarios in MPI-GE (Maher et al. 2019) over 2020–2050 for both JJA 200-hPa geopotential height (Z200) and September sea ice concentration (SIC) within the Arctic (poleward of 60°N). Second, we remove the ensemble mean trend from each member, so the residual trends only reflect internal variability of the model over the 31 years. We then use SMCA between JJA Z200 and September SIC trend fields across all the members in a given scenario. The leading ensemble-based SMCA modes reflect the dominant coupled patterns of internally-generated trends in Z200 and SIC. For comparison, we also calculate the September sea ice area (SIA) trends in each member. We note, that a similar approach, using ensemble member trend-based EOFs, has previously been presented in Wettstein and Deser (2014) to study co-variability of atmospheric circulation and sea ice.

The extent to which the SIA trends resemble the time expansion coefficients of SMCA in each member can be used to probe the degree of linearity in the coupling between Z200 and SIC in a given RCP scenario. In the case

of the RCP4.5 scenario, nearly half of the members in the fast melting group (15% of the members with strongest sea ice melt) show identically strong sea ice melt despite the linear decrease in the time expansion coefficient series of the same members (Figure 3d). Such a phenomenon is not observed under the RCP2.6 and 8.5 scenarios (Figure 3a,g), which suggests that the coupling may exhibit stronger non-linearity under the RCP4.5 scenario. We also show that the spatial patterns of Z200 and SIC corresponding to the leading ensemble-based SMCA mode differs slightly between RCP4.5 and the two other

forcing scenarios, indicating some role for the intensity of external forcing, which remains a subject of future work (Figure 3b-c, e-f, h-i). Interestingly, the shared fraction of co-variance between Z200 and SIC (indicated in the panel titles in Figure 3) are also slightly higher for the RCP4.5 scenario compared to the other two. Regarding the physical mechanism behind the observed co-variability between atmospheric circulation and sea ice, we argue based on previous work (Ding et al. 2017; Baxter et al. 2019) that an internal atmospheric process manifested as a high-pressure driven adiabatic warming (via regulating downward longwave radiation) can cause sea ice melt on top of the externally forced melting (Figures 3b-c, e-f, h-i). A more thorough discussion of this physical mechanism and its limited representation in SMILEs can be found in Topál et al. (2020).

Outlook

We have applied the mathematically well-established “snapshot view” based on dynamical systems theory to the analysis of SMILEs and reconsidered traditional methodologies to study possible future changes in internal variability. A future direction of the research

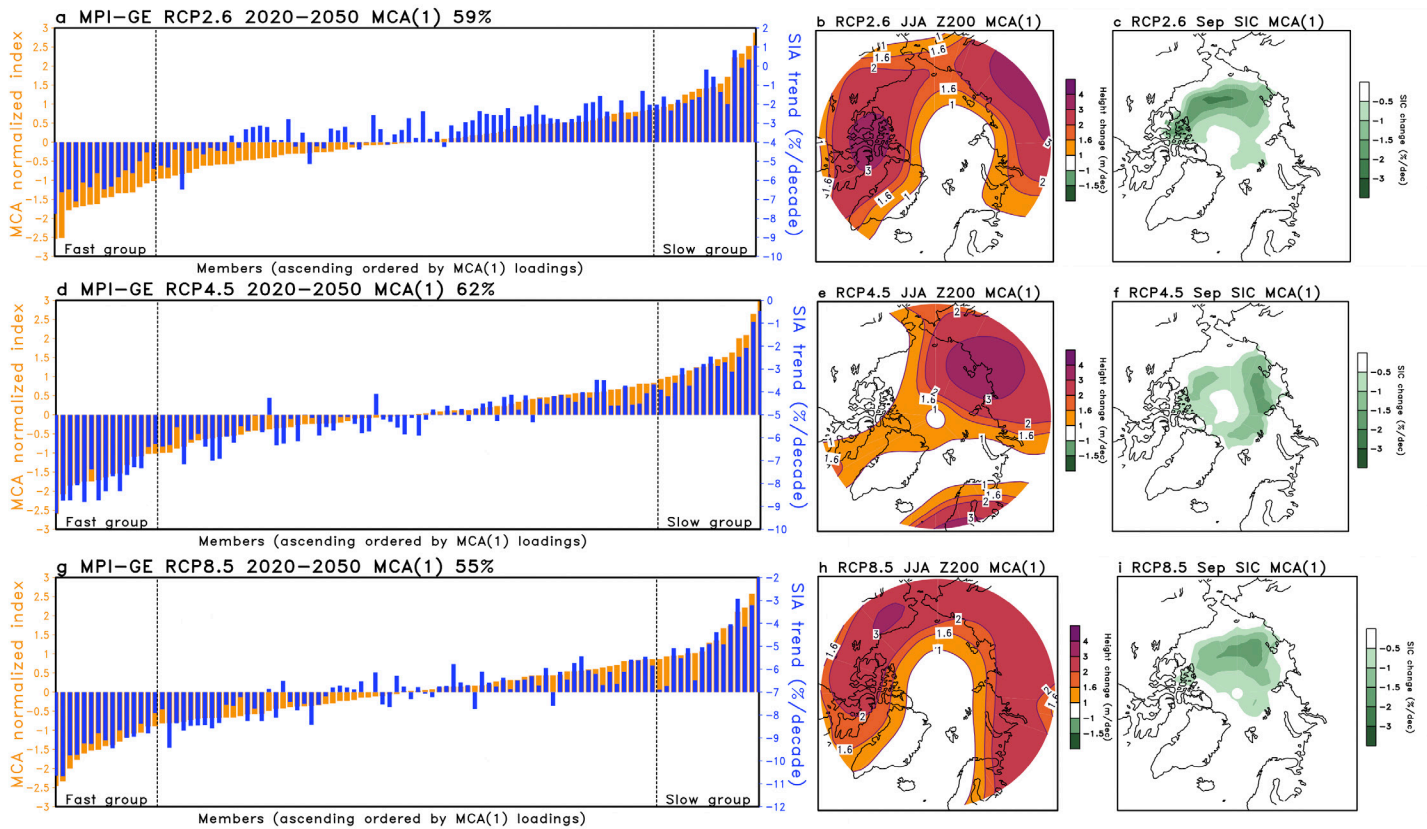


Figure 3. Snapshot maximum covariance analysis (SMCA) between June-July-August Z200 and September sea ice concentration (SIC) trends during 2020–2050 in the three RCP scenarios (2.6, 4.5 and 8.5) from the MPI-GE. The bar plots on the left represent the normalized member loadings (orange bars: left y axis) of the leading SMCA mode and the corresponding members' September total sea ice area (SIA) trends (blue bars: right y axis), arranged in ascending order of the SMCA loadings. The percentages represent the shared fraction of covariance between Z200 and SIC trends across each ensemble explained by the leading mode. Maps in the middle and right columns show the Z200 and SIC spatial patterns, respectively, of the leading SMCA mode for each scenario.

could be comparing SEOF results to observations. One might try a comparison using carefully chosen (but still subjective) multiple time windows centered to the instantaneous SEOF year to construct the relevant traditional EOF pattern using a single time series. However, this comparison is expected to yield similar results only if the external forcing does not change much within the chosen time window and, therefore, ergodicity approximately holds. Equally, it is to be noted that the ongoing climate change is not ergodic (Tél et al. 2019). As a consequence, the above-mentioned comparison

can serve as a measure of the ergodicity as well. A crucial message of the snapshot view is that all of the traditional, time series-based methods can be reformulated for ensembles, which will be of use for the broader climate community. In this way, utilizing ensemble-based (snapshot) analyses of the available SMILEs, ambiguous results arising from subjective choices of traditional methods (e.g. length and center of time windows) can be avoided, the possible climate states at each time instant can be properly characterized, and forced changes in any ensemble-based quantity can be determined.

Acknowledgments

This article was supported by the ÚNKP-18-4 (T.H.) and ÚNKP-19-3 (D.T.) New National Excellence Program of the Ministry for Innovation and Technology, by grant NTP-NFTÖ-18 (D.T.) of the Ministry of Human Capacities, by the János Bolyai Research Scholarship of the Hungarian Academy of Sciences (T.H., M.H.), and by the National Research, Development and Innovation Office–NKFIH under Grants PD-121305 and PD-132709 (T.H.), PD-124272 (M.H.), FK-124256 and K-125171 (T.H., M.H.). The authors are thankful to the developer group of MPI-GE for providing the MPI-GE ensembles and wish to thank the Climate Data Gateway at NCAR for providing access to the output of the CESM-LE.

The authors acknowledge and especially thank Gábor Drótos, Tamás Bódai and János Márffy for establishing the fundamentals of applying snapshot attractors theory to climate dynamics, including early stages of their SEOF-related research. The authors are grateful to Tamás Tél for inspiring ideas and suggestions on the subject of the section Theoretical background.

References

- Barnes, E. A. and L. Polvani, 2013: Response of the midlatitude jets, and of their variability, to increased greenhouse gases in the CMIP5 models. *J. Climate*, **26**, 7117–7135, doi:10.1175/JCLI-D-12-00536.1.
- Baxter, I., and Coauthors, 2019: How tropical Pacific surface cooling contributed to accelerated sea ice melt from 2007 to 2012 as ice is thinned by anthropogenic forcing. *J. Climate*, **32**, 8583–8602, doi:10.1175/JCLI-D-18-0783.1.
- Bódai T., and T. Tél, 2002: Annual variability in a conceptual climate model: Snapshot attractors, hysteresis in extreme events, and climate sensitivity. *Chaos*, **22**, 023110, doi:10.1063/1.3697984.
- Bódai, T., G. Drótos, M. Herein, F. Lunkeit, and V. Lucarini, 2020: The forced response of the El Niño–Southern Oscillation–Indian Monsoon teleconnection in ensembles of Earth system models. *J. Climate*, **33**, 2163–2182, doi:10.1175/JCLI-D-19-0341.1.
- Bretherton, C. S., C. Smith, and J. M. Wallace, 1992: An intercomparison of methods for finding coupled patterns in climate data. *J. Climate*, **5**, 541–560, doi:10.1175/1520-0442(1992)005<0541:AIOMFF>2.0.CO;2.
- Chekroun M. D., E. Simonnet, and M. Ghil, 2011: Stochastic climate dynamics: Random attractors and time dependent invariant measures. *Phys. D*, **240**, 1685, doi:10.1016/j.physd.2011.06.005.
- Deser, C., A. Phillips, V. Bourdette, H. Teng, 2012: Uncertainty in climate change projections: the role of internal variability. *Clim. Dyn.* **38**, 527–546, doi:10.1007/s00382-010-0977-x.
- Deser, C., and Coauthors, 2020: Insights from Earth system model initial-condition large ensembles and future prospects. *Nat. Clim. Change*, **10**, 277–286, doi:10.1038/s41558-020-0731-2.
- Ding, Q., and Coauthors, 2019: Fingerprints of internal drivers of Arctic sea ice loss in observations and model simulations. *Nat. Geosci.*, **12**, 28–33, doi:10.1038/s41561-018-0256-8.
- Ding, Q., and Coauthors, 2017: Influence of high-latitude atmospheric circulation changes on summertime Arctic sea ice. *Nat. Climate Change*, **7**, 289–295, doi:10.1038/nclimate3241.
- Drótos, G., T. Bódai, and T. Tél, 2015: Probabilistic concepts in a changing climate: snapshot attractor picture. *J. Climate*, **28**, 3275–3288, doi:10.1175/JCLI-D-14-00459.1.
- Ghil M, M. D. Chekroun, and E. Simonnet, 2008: Climate dynamics and fluid mechanics: Natural variability and related uncertainties. *Phys. D*, **237**, 2111, doi:10.1016/j.physd.2008.03.036.
- Haszpra, T., M. Herein, and T. Bódai, 2020a: Investigating ENSO and its teleconnections under climate change in an ensemble view – a new perspective. *Earth Syst. Dyn.*, **11**, 267–280, doi:10.5194/esd-11-267-2020.
- Haszpra, T., D. Topál, and M. Herein, 2020b: On the time evolution of the Arctic Oscillation and related wintertime phenomena under different forcing scenarios in an ensemble approach. *J. Climate*, **33**, 3107–3124, doi:10.1175/JCLI-D-19-0004.1.
- Hawkins, E., and R. Sutton, 2009: The Potential to Narrow Uncertainty in Regional Climate Predictions. *Bull. Amer. Meteor. Soc.*, **90**, 1095–1108, doi:10.1175/2009BAMS2607.1.
- Hawkins, E., D. Frame, L. Harrington, M. Joshi, A. King, M. Rojas, R. Sutton, 2020: Observed emergence of the climate change signal: from the familiar to the unknown. *Geophys. Res. Lett.*, **47**, e2019GL086259, doi:10.1029/2019GL086259.
- Herein M., G. Drótos, T. Haszpra, J. Márffy, and T. Tél, 2017: The theory of parallel climate realizations as a new framework for teleconnection analysis. *Sci. Rep.* **7**, 44529, doi:10.1038/srep44529.
- Herein, M., J. Márffy, G. Drótos, and T. Tél, 2016: Probabilistic concepts in intermediate-complexity climate models: A snapshot attractor picture. *J. Climate*, **29**, 259–272, doi:10.1175/JCLI-D-15-0353.1.
- Kay, J. E., and Coauthors, 2015: The Community Earth System Model (CESM) Large Ensemble Project: A community resource for studying climate change in the presence of internal climate variability. *Bull. Amer. Meteor. Soc.*, **96**, 1333–1349, doi:10.1175/BAMS-D-13-00255.1.
- Ku, W. L., M. Girvan, and E. Ott, 2015: Dynamical transitions in large systems of mean field-coupled Landau-Stuart oscillators: Extensive chaos and cluster states. *Chaos*, **25**, 123122, doi:10.1063/1.4938534.
- Lehner, F., C. Deser, N. Maher, J. Marotzke, E. M. Fischer, L. Brunner, R. Knutti, E. Hawkins, 2020: Partitioning climate projection uncertainty with multiple large ensembles and CMIP5/6. *Earth Syst. Dyn.*, **11**, 491–508, doi:10.5194/esd-11-491-2020.

